Subunit regulation of the neuronal α_{1A} Ca^{2+} channel expressed in *Xenopus* oocytes

Michel De Waard and Kevin P. Campbell*

Howard Hughes Medical Institute, Department of Physiology and Biophysics, University of Iowa, College of Medicine, Iowa City, IA 52242, USA

1. Voltage-dependent Ca^{2+} channels are multi-protein complexes composed of at least three subunits: α_1, $\alpha_2\delta$ and β. Ba^{2+} currents were recorded in *Xenopus* oocytes expressing the neuronal α_{1A} Ca^{2+} channel, using the two-electrode voltage-clamp technique. Various subunit combinations were studied: α_{1A}, $\alpha_{1A}\alpha_2\delta_b$, $\alpha_{1A}\beta$ or $\alpha_{1A}\alpha_2\delta_b\beta$.

2. The α_{1A} subunit alone directs the expression of functional Ca^{2+} channels. It carries all the properties of the channel: gating, permeability, voltage dependence of activation and inactivation, and pharmacology. The α_{1A} channel is activated by low voltages when physiological concentrations of the permeant cation are used. Both ancillary subunits $\alpha_2\delta$ and β induced considerable changes in the biophysical properties of the α_{1A} current. The subunit specificity of the changes in current properties was analysed for all four β gene products by coexpressing β_{1b}, β_{2a}, β_3 and β_4.

3. All β subunits induce a stimulation in the current amplitude, a change in inactivation kinetics, and two hyperpolarizing shifts – one in the voltage dependence of activation and a second in the voltage dependence of steady-state inactivation. The most significant difference in regulation among β subunits is the induction of variable rate constants of current inactivation. Rates of inactivation were induced in the following order (fastest to slowest): $\beta_3 > \beta_{1b} = \beta_4 > \beta_{2a}$.

4. The $\alpha_2\delta_b$ subunit does not modify the properties of α_{1A} Ca^{2+} channels in the absence of β subunits. However, this subunit increases the β-induced stimulation in current amplitude and also regulates the β-induced change in inactivation kinetics.

5. Of all the subunit combinations tested, Ca^{2+} channels that included a β subunit were the most prone to decrease in activity. It is concluded that β subunits are the primary target for the inhibitory mechanisms involved in Ca^{2+} channel run-down.

6. Both $\alpha_2\delta_b$ and β_{1b} subunits slightly modified the sensitivity of the α_{1A} subunit to the snail peptide ω-conotoxin MVIIC.

7. The subunit-induced changes in properties of the α_{1A} channel are surprisingly similar to changes reported for other α_1 subunits. These modifications in channel activity should therefore represent important functional landmarks in the on-going characterization of subunit—subunit interactions.

Voltage-dependent Ca^{2+} channels are well characterized on the basis of their biophysical and pharmacological properties. At least three types of high-voltage-activated Ca^{2+} channels, termed L-, N- and P-type, have been differentiated by their sensitivities to various neurotoxins and organic Ca^{2+} channel modulators (Miller, 1992). The purified rabbit skeletal muscle L-type channel is composed of four subunits: the α_1 pore-forming subunit, which contains the binding sites for all C^{2+} channel modulators affecting this channel type; the $\alpha_2\delta$ subunit, a disulphide-linked dimer; the transmembrane γ subunit and the intracellular β subunit (Takahashi, Seagar, Jones, Reber & Catterall, 1987). The primary structures of all the subunits composing this L-type Ca^{2+} channel were deduced by cloning (Tanabe *et al.* 1987; Ellis *et al.* 1988; Ruth *et al.* 1989; Jay *et al.* 1990). By using these cDNA sequences a

* To whom correspondence should be addressed.

probes, it was found that as many as six different genes coded for each α_1, β and $\alpha_2\delta$ subunit (Tanabe *et al.* 1987; Ellis *et al.* 1988; Mikami *et al.* 1989; Ruth *et al.* 1989; Hui, Ellinor, Krizanova, Wang, Diebold & Schwartz, 1991; Mori *et al.* 1991; Dubel *et al.* 1992; Niidome, Kim, Friedrich & Mori, 1992; Perez-Reyes *et al.* 1992; Castellano, Wei, Birnbaumer & Perez-Reyes, 1993*a*, *b*). Also, additional molecular diversity arises from alternative splicing of transcripts of these distinct genes. In spite of this remarkable diversity, all these subunits have conserved structural features. β subunits are all capable of binding to a single amino acid motif that is present on all α_1 subunite cloned so far (Pragnell, De Waard, Mori, Tanabe, Snutch & Campbell, 1994). It was also found that the $\alpha_2\delta$ subunit is conserved in a wide range of organs (Ellis *et al.* 1988; Morton & Froehner, 1989). For instance, cloning and sequencing of a cDNA encoding a rat brain $\alpha_2\delta$ subunit shows 95% amino acid identity with an alternative splice variant expressed in skeletal muscle (Kim, Kim, Lee, King & Chin, 1992). More recently, the brain N-type Ca^{2+} channel was also purified (Witcher *et al.* 1993) and reconstituted into bilayers (De Waard, Witcher & Campbell, 1994). Despite their differing cellular functions, the N-type Ca^{2+} channel bears remarkable structural and functional homologies with the L-type channel. This channel is composed of structurally similar subunits (α_{1B}, $\alpha_2\delta_b$, β_3 for the N-type *versus* α_{1S}, $\alpha_2\delta_b$, β_{1a} for the L-type) although it differs by the presence of a fourth subunit (a 95 kDa protein *versus* γ subunit in the L-type channel). Expression experiments provide further evidence that the core subunit composition of all voltage-dependent Ca^{2+} channels could be minimally described by $\alpha_1\alpha_2\delta\beta$. Coexpression of various β subunits with all classes of α_1 subunits (S, A, B, C, D and E if one adopts the most recent acknowledged nomenclature; Birnbaumer *et al.* 1994) results in enhanced current amplitude (Mori *et al.* 1991; Hullin *et al.* 1992; Williams *et al.* 1992*a, b*; Ellinor et al. 1993) and/or altered voltage dependence and kinetics of the resulting Ca^{2+} channels (Lacerda *et al.* 1991; Singer, Biel, Lotan, Flockerzi, Hofmann & Dascal, 1991; Varadi, Lory, Schultz, Varadi & Schwartz, 1991; Soong, Stea, Hodson, Dubel, Vincent & Snutch, 1993). There are actually fewer experimental data illustrating the regulation of Ca^{2+} channel currents by the $\alpha_2\delta$ subunit. However, it has been demonstrated that this subunit contributes to a normalization of the activation and inactivation kinetics of the α_{1C} subunit (Table 2). Altogether, these observations prompted us to determine how various α_1 subunits correlate among each other by isolating common functional features. Conserved subunit regulation among α_1 subunits should provide some insights into the structural determinants involved in subunit–subunit interactions of Ca^{2+} channels. To reach this goal, we chose to study the subunit regulation of the α_1 Ca^{2+} channel since the characterization of this neuronal channel is still very fragmentary. *Xenopus* oocytes were used because (1) these cells have been an expression system of choice for Ca^{2+} channels and (2) they express only low levels of endogenous voltage-gated Na^+, K^+ and Ca^{2+} channels (Dascal, 1987). This report is therefore the first detailed description of the biophysical and pharmacological properties of the α_{1A} subunit expressed by itself. Comparisons between the properties of α_{1A} Ca^{2+} channels on the one hand and $\alpha_{1A}\alpha_2\delta$, $\alpha_{1A}\beta$ or $\alpha_{1A}\alpha_2\delta\beta$ Ca^{2+} channels on the other demonstrate that contrary to an initial report by Mori *et al.* (1991), but consistent with the expression of other α_1 subunits, both ancillary subunits $\alpha_2\delta$ and β have dramatic effects on the activity of the α_1 Ca^{2+} channel.

METHODS

Preparation of *Xenopus* oocytes

Mature *Xenopus laevis* female frogs were purchased from NASCO (WI, USA). The animals were maintained under a 12 h light–12 h dark cycle at 16 °C. To harvest oocytes, the frogs were anaesthetized to full immobility with 0·03% ethyl *p*-amino-benzoate (Sigma) and their ovaries were surgically removed. The incision created was sutured immediately after removal of the oocytes and the animals returned to the tank following recovery from surgery. They were then allowed to recover for at least 2 months before being reused. Follicle membranes from isolated oocytes were enzymatically digested for 2 h with 2 mg ml^{-1} of collagenase (Type IA, Sigma) in Ca^{2+}-free Earth's solution (Table 1). After defoliculation, oocytes at stages V and VI were isolated and washed several times with Ca^{2+}-free and subsequently standard Earth's solution (Table 1). The oocytes were then incubated overnight at 18 °C in Earth's solution before RNA injections.

cRNA synthesis and injection into oocytes

In vitro transcription was performed in a volume of 25 μl containing the following (mM): 40 Tris-HCl, 50 NaCl, 8 $MgCl_2$, 2·5 spermidine, 30 dithiotreitol, 0·4 ribonucleotides, 0·3 Capanalog $m^7G(5')ppp(5')G$, 1 μg of linearized and proteinase K-treated DNA template, and 10 units of T7 RNA polymerase (Stratagene, La Jolla, CA, USA; for the synthesis of the $\alpha_2\delta_b$ and β subunits) or 20 units of SP6 RNA polymerase (Promega, Madison, WI, USA; for the synthesis of the α_{1A} subunit) (pH 7·5). The mixture was incubated at 37 °C for 60 min, then resupplemented for an additional 30 min with 10 or 20 units of T7 or SP6 RNA polymerase, respectively. At the end of the reaction, the DNA template was digested for 10 min with 10 units of DNase I. After phenol/chloroform extraction and ethanol precipitation, the cRNA product was resuspended in 150 mM KCl. Fifty nanolitres of various *in vitro* transcribed RNA mixtures (0·5 $\mu g\ \mu l^{-1}$ α_{1A}, 0·5 $\mu g\ \mu l^{-1}$ $\alpha_1\delta_b$ and/or 0·2 $\mu g\ \mu l^{-1}$ β) were injected per oocyte. After injection, the oocytes were maintained for 4-6 days at 16 °C in defined nutrient oocyte medium (Eppig & Dumont, 1976) supplemented with 50 $\mu g\ ml^{-1}$ gentamycin. Only oocytes expressing Ba^{2+} currents higher than 50 nA were included in the analysis. When present, endogenous Ba^{2+} currents never exceeded 10 nA (n = 8). These currents were not significantly stimulated by expression of the $\alpha_2\delta_b$ subunit (n = 7) and reached, on average, less than 60 nA upon expression of β subunits (n=10) or $\alpha_2\delta_b\beta$ subunit combinations (n = 5).

Table 1. Composition of the solutions used in this study

Solution	Na^+	K^+	Ca^{2+}	Ba^{2+}	Mg^{2+}	Cl^-	SO_4^{2-}	HCO_3^-	Hepes	Niflumic acid
BS (Ca^{2+} free)	90·4	1	–	–	0·82	89	0·82	2·4	15	–
BS (standard)	90·4	1	2	–	0·82	93	0·82	2·4	15	–
Ba-40	50	2	–	40	–	2	–	–	5	1
Ba-30	60	2	–	30	–	2	–	–	5	1
Ba-20	70	2	–	20	–	2	–	–	5	1
Ba-10	80	2	–	10	–	2	–	–	5	1
Ba-5	85	2	–	5	–	2	–	–	5	1
Ba-2	90	2	–	2	–	2	–	–	5	1
Ba-1	93	2	–	1	–	2	–	–	5	1
Ba-0	93	2	–	0	–	2	–	–	5	1

All concentrations are in mM. The solutions were titrated to pH 7·4 with NaOH (Barth's solution, BS) or with methanesulphonic acid (barium solutions). EGTA (0·1 mM) was added to Ba-0 to effectively buffer all free divalent cations. Niflumic acid was obtained from Sigma.

Electrophysiological recordings and data analysis

The experiments were performed at room temperature (20–22 °C) using the Ba^{2+} solutions listed in Table 1. Two-electrode voltage clamp was performed using a Dagan TEV-200 amplifier (Dagan Instruments, Minneapolis, MN, USA). For bath applications of ω-CgTX MVIIC, 1 mg ml^{-1} of cytochrome *c* was added to the external Ba^{2+} solution to saturate non-specific binding sites. Control experiments demonstrate that cytochrome c has no effect on channel activity at this concentration (data not shown). Microelectrodes were filled with 3 M KCl and had resistances between 0·5 and 2 MΩ. The bath solution was clamped to a reference potential of 0 mV. The membrane current was permanently monitored and we considered only the oocytes for which there was less than 10% fluctuation in leak current amplitude during the time course of the experiment. Records were filtered at 400 Hz and sampled at 2 kHz. Leak and capacitance currents were subtracted on-line by a hyperpolarizing prepulse protocol (P/6). If present, residual capacitance was blanked. Voltage pulses were delivered for 500 ms every 10 s (activation protocols) or 30 s (steady-state inactivation protocols). Data were analysed using pCLAMP version 5·5 (Axon Instruments). Fits of *I–V* curves were obtained assuming an activation curve of a Boltzmann type:

$$I_{Ba} = [g(V_t - E)] / [1 + \exp(-(V_t - V_{½})/k)],$$

where V_t represents the test potential, g the maximum conductance, E the apparent reversal potential, $V_{½}$ the potential of half-activation, and k the range of potential responsible for an e-fold change around $V_{½}$. The steady-state inactivation curves were also described by a Boltzmann-type equation:

$$I_{Ba} = \{1 + \exp[(V - V_{½})/k)]\} - 1,$$

where the current amplitude I_{Ba} has decreased to a half-amplitude at $V_{½}$ with an e-fold change over k mV. Steady-state inactivation protocols lasted 7 min. For the analysis of the activation and inactivation data, cells that had significant run-down were discarded. Run-down was assessed by the irreversible decrease in current amplitude with time. All values are means ± S.E.M. Our analyses are based on recordings from a total of $n = 206$ oocytes.

cDNA clones

cDNA clones used for expression were pSPCBI-2 (α_{1A} subunit from Mori *et al.* 1991; gene bank accession number X57477), $\alpha_2\delta_b$ (T. P. Snutch, unpublished sequence; accession number M86621), β_{1b}, (Pragnell, Sakamoto, Jay & Campbell, 1991; accession number X61394), β_2 (Hullin *et al.* 1992; accession number X64297), β_3 (Dr D. R. Witcher, unpublished sequence; accession number M88751) and β_4 (Castellano *et al.* 1993*b*; accession number L02315).

RESULTS

The α_{1A} subunit directs the expression of functional Ca^{2+} channels, the properties of which are not regulated by the $\alpha_2\delta_b$ subunit

Expression of α_1 subunits generally results in low current density (Mori *et al.* 1991; Singer *et al.* 1991; Stea *et al.* 1993; Tomlinson, Stea, Bourinet, Charnet, Nargeot & Snutch, 1993). In many cases, the current densities are in fact so low that accurate biophysical descriptions of α_1 Ca^{2+} channels cannot be performed unless β subunits are coexpressed (Mori *et al.* 1991; Williams *et al.* 1992*b*; Ellinor *et al.* 1993). We increased the expression levels of the α_{1A} subunit by selecting *Xenopus* frog donors that yielded oocytes capable of high expression levels. To saturate translation levels, these cells were injected at cRNA concentrations higher than previously reported for this channel (Mori *et al.* 1991; Sather, Tanabe, Zhang, Mori, Adams & Tsien, 1993). Since high concentrations of permeant ion increase the resolution of Ca^{2+} current, the recordings were also performed with 40 mM external Ba^{2+} as the charge carrier unless otherwise stated. We also estimated the peak level of Ca^{2+} channel expression at 4–6 days after cRNA injection.

Under these optimized conditions, we found that expression of the α_{1A} subunit results in a very significant inward current. The maximum mean current amplitude was reached at 20 mV with I_{Ba} of –269 ± 66 nA ($n = 4$). This was much larger than the mean endogenous Ca^{2+} current (< 10 nA). This rather high level of expression therefore allowed a more systematic characterization of α_{1A} Ca^{2+} channels in the absence of the auxiliary subunits.

Activation of the α_{1A} Ca^{2+} channel current started at –20 mV, experimentally peaked at +20 mV and reversed at 53 mV (Fig. 1*A*). A fit of the data with a modified Boltzmann equation estimated the peak current more precisely at 17·5 ± 0·9 mV. Ba^{2+} current activated quickly and reached peak amplitude in 9 ± 1 ms (n = 4) at 20 mV (data not shown). Coexpression of the $\alpha_2\delta_b$ subunit with the α_{1A} Ca^{2+} channel did not significantly modify the mean current amplitude or the voltage dependence of activation. The maximal inward current of $\alpha_{1A}\alpha_2\delta_b$ was of a similar amplitude to the α_{1A} Ca^{2+} channel with –289 ±141 nA at 20 mV. Also, the current peaked at about 17·6 ± 0·6 mV (n = 16), which was similar to the peak for α_{1A} Ca^{2+} channels.

The voltage dependence of the steady-state inactivation of α_{1A} Ca^{2+} channels was also determined. The data show that the inactivation of this channel occurred at fairly depolarized values over a 40 mV interval. The mid-point of inactivation occurred at –46± 1·2mV (n = 5) (Fig. 1*B*). As for the activation, the coexpression of the $\alpha_2\delta_b$ subunit did not significantly modify the voltage dependence of inactivation of the α_{1A} channel. As for α_{1A} Ca^{2+} channels, the estimated half-inactivation potential of $\alpha_{1A}\alpha_2\delta_b$ channels was –42 ± 2 mV (n = 4).

During sustained membrane depolarization, the current amplitude of α_{1A} Ca^{2+} channels progressively decayed as a result of the inactivation of the channel. We found that the time course of this inactivation consisted of two kinetic components. At 20 mV, for instance, the first inactivating component of α_{1A} Ca^{2+} channels follows a fast time constant, τ_1, of 27 ± 0·7 ms (n = 4) that constitutes 30% of the total inactivating current. The second inactivating component was represented by a slower time constant, τ_2, of 355 ± 16 ms and constituted the remaining 70% of the inactivating current (Fig. 1*C*). The slow inactivating component was the most voltage sensitive. The time constant of inactivation increased by a factor of 3·1 between depolarizing pulses of 0 and 50 mV. In comparison, the fast inactivating component increased by 1·4-fold over the same range of potentials. In contrast, the ratio of current amplitude of these components was only slightly voltage dependent (not shown). The fast inactivating component, which equalled 32% of the total inactivating current at 0 mV, still represented 25% of the current at 40 mV. Again, as for the voltage dependence of activation and inactivation, the expression of the $\alpha_2\delta_b$ subunit did not modify the inactivation kinetics of the α_{1A} Ca^{2+} channel.

We ensured that both components, and in particular the fast inactivating current, were carried by the α_{1A} Ca^{2+} channel. Several experimental observations demonstrated that this component was indeed not supported by endogenous Ca^{2+} channels normally present in oocytes. (1) In the absence of β and $\alpha_2\delta_b$ subunits, the endogenous current was less than 10 nA in every case (n=8). In comparison, the fast component of the inactivating current of the α_{1A} Ca^{2+} channel reached an estimated current amplitude of 90 nA. (2) The ratio of fast and slow current amplitudes remained constant from oocyte to oocyte and was independent of the total current amplitude recorded. This would not be expected if slow and fast components were carried by different Ca^{2+} channels. (3) Both components were irreversibly blocked by ω-CgTX MVIIC (not shown). This twenty-six amino acid toxin, isolated from the marine snail *Conus magus* (Hillyard *et al.* 1992), is a potent and complete blocker of the currents carried by the $\alpha_{1A}\alpha_2\delta_b\beta$ Ca^{2+} channel (Sather *et al.* 1993) and is not known to affect the endogenous current. (4) Despite the presence of two distinct kinetic components, the Ba^{2+} current activated and inactivated along a single voltage component (Fig. 1). Again, this would not be expected if a significant fraction of the current was carried by the endogenous channel. For instance, Ba^{2+} currents through endogenous channels peak at 30 mV, which is at least 10 mV more depolarized than the peak for α_{1A} Ca^{2+} channels. The presence of this channel would therefore be detected by a bend in the current–voltage relationship.

β subunits induce four major modifications of the biophysical properties of the α_{1A} channel, two of which are modulated by the α_2/δ_b subunit

As previously done for the $\alpha_2\delta_b$ subunit, we monitored the effects of β subunits on the amplitude, voltage dependence and kinetics of α_{1A} Ca^{2+} channel currents. We found that β subunits modified all of these properties. We also demonstrated that the $\alpha_2\delta_b$ subunit regulated two of the four major modifications induced by β subunits.

Expression of the β_{1b}, subunit resulted in a hyperpolarizing shift in the voltage dependence of α_{1A} Ca^{2+} channel activation (Fig. 2*Aa*). For instance, the estimated peak current of $\alpha_{1A}\beta_{1b}$ occurred at –0·5 ± 1·4mV (n = 11) which, when compared with α_{1A} Ca^{2+} channels, corresponded to a 17 ± 1 mV shift towards hyperpolarized potentials. Overall, the shift in peak current was due to a lower threshold potential (–30 instead of –20 mV) and a steeper voltage dependence (k=3·8 ± 0·3 instead of 7·6 ± 0·3 mV for the α_{1A} Ca^{2+} channels). Expression of both $\alpha_2\delta_b$ and β_{1b} subunits did not modify the amplitude of this hyperpolarizing shift. On average, the shift induced by β_{1b}, equalled 15 ± 3 mV in the presence of $\alpha_2\delta_b$ (n= 13, Fig.2*Ab*). Interestingly, all β subunits induced hyperpolarizing shifts in the current—voltage relationship of $\alpha_{1A}\alpha_2\delta_b$, with, however, some minor quantitative differences (Fig.2*Ab*). The mean shifts in peak values were 7·5 ± 2·3 mV ($\alpha_{1A}\alpha_2\delta_b\beta_{2a}$, n=8), 9·5 ± 2·2 mV ($\alpha_{1A}\alpha_2\delta_b\beta_3$, n = 8) and 17·5 ± 2 mV ($\alpha_{1A}\alpha_2\delta_b\beta_4$, n = 9). We classified the β subunits according to their abilities to shift the voltage dependence of activation with $\beta_4 = \beta_{1b} > \beta_3 = \beta_{2a}$.

Expression of β subunits also resulted in a considerable stimulation of the peak current of the α_{1A} Ca^{2+} channel.

The maximum current amplitude of $\alpha_{1A}\beta_{1b}$ Ca^{2+} channel was –1955 ± 230 nA (n = 11) at 0 mV (Fig.2*Ba*). This corresponds to a mean β_{1b}, stimulation of (7·3 ± 1·2)-fold (n = 15). Although the $\alpha_2\delta_b$ subunit did not itself affect the current amplitude of α_{1A} Ca^{2+} channels (mean current amplitudes, –269 and –289 nA for α_{1A} and $\alpha_{1A}\alpha_2\delta_b$ Ca^{2+} channels, respectively), expression of $\alpha_2\delta_b$ did increase the β_{1b} stimulation further by a factor of 2·5 and brought the

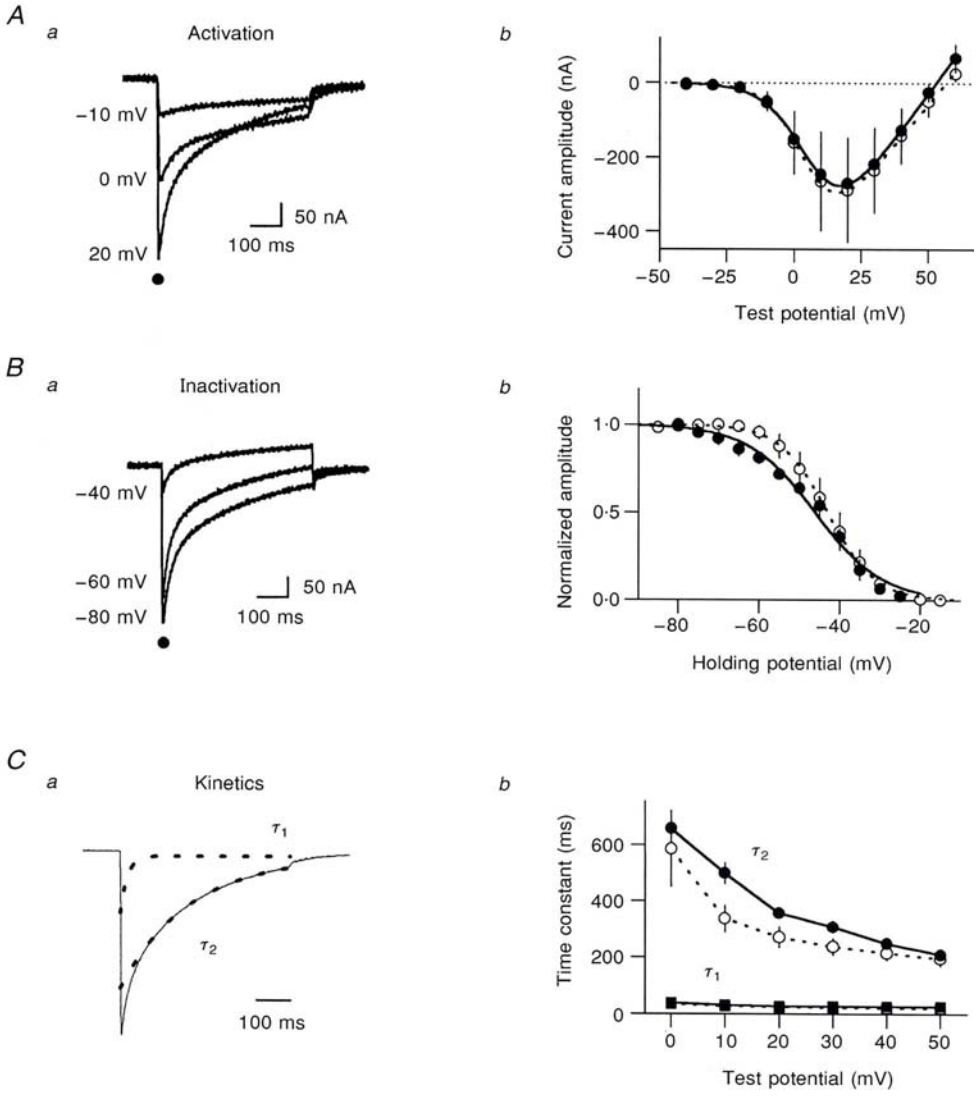

Figure 1. Properties of α_{1A} current and absence of regulation by the $\alpha_2\delta_b$ subunit

A, voltage dependence of activation and effect of $\alpha_2\delta_b$. *Aa*, trace examples of Ba^{2+} current activation at –10, 0 and 20 mV test pulses. Holding potential is –90 mV. *Ab*, average current-voltage relationship for α_{1A} (n = 4, ●, continuous line) and $\alpha_{1A}\alpha_2\delta_b$ currents (n = 16, ○, dashed line). Test pulses were delivered by 10 mV increments. Error bars are S.E.M. Fits of the average activation data yield g = 9·9 or 8·8 μS, E= 52·8 or 56·6 mV, $V_{½}$= 7·4 or 5·5 mV and k = 7·7 or 6·9 mV without or with $\alpha_2\delta_b$ coexpression, respectively. *B*, voltage dependence of inactivation and effect of $\alpha_2\delta_b$. *B a*, trace examples of α_{1A} Ba^{2+} current at holding potentials of –80, –60 and –40 mV to show the reduction in current amplitude by steady-state inactivation. *Bb*, average steady-state inactivation curve for α_{1A} (●, continuous line) and $\alpha_{1A}\alpha_2\delta_b$ currents (○, dashed line). Peak current amplitudes were normalized to the maximum current amplitude reached during the protocol. Normalized current amplitudes were then averaged and plotted as a function of holding potential. Fits to the average data yield $V_{½}$ = –46 or –42 mV and k= 8·3 or 6·1 mV without or with $\alpha_2\delta_b$ coexpression, respectively. Data are the means ± S.E.M. of n = 5 (–$\alpha_2\delta_b$ and n = 4 (+$\alpha_2\delta_b$) oocytes. *C*, kinetics of inactivation and effect of $\alpha_2\delta_b$. *Ca*, trace example at 30 mV test potential and decomposition of the inactivating current into two components (dashed line). *Cb*, plot of the two time constants τ_1 and τ_2 as a function of test potential for α_{1A} (filled symbols, continuous lines) or for $\alpha_{1A}\alpha_2\delta_b$ inactivating currents (open symbols, dashed lines).

final mean current to –5272 ± 762 nA (n = 13). This $\alpha_2\delta_b$ potentiation provided a total stimulation of (18·2 ± 6·6)-fold by β_{1b}. The stimulation in current amplitude and the potentiation in stimulation by the $\alpha_2\delta_b$ subunit could be observed upon expression of any of the four β subunits. However, the β subunits differed in their ability to stimulate the current. The mean stimulations were 5·38 ± 2·1 (β_{2a}), 5·48 ± 2·1 (β_3) and 19·3 ± 7·8 (β_4). We therefore also classified the β subunits according to their stimulation efficiencies with $\beta_4 = \beta_{1b} > \beta_3 = \beta_{2a}$. As a result of the shift in voltage dependence of activation, the stimulation of current amplitude induced by β subunits was larger at hyperpolarized potentials (Fig. 2 *B b*). For instance, expression of both β_{1b} and $\alpha_2\delta_b$ resulted in an (87 ± 42)-fold stimulation of α_{1A} current amplitude when measured at 0 mV. In contrast, when the current was measured at 30 mV, this stimulation was on average six times smaller with a (14 ± 5)-fold enhancement in amplitude. A lower but

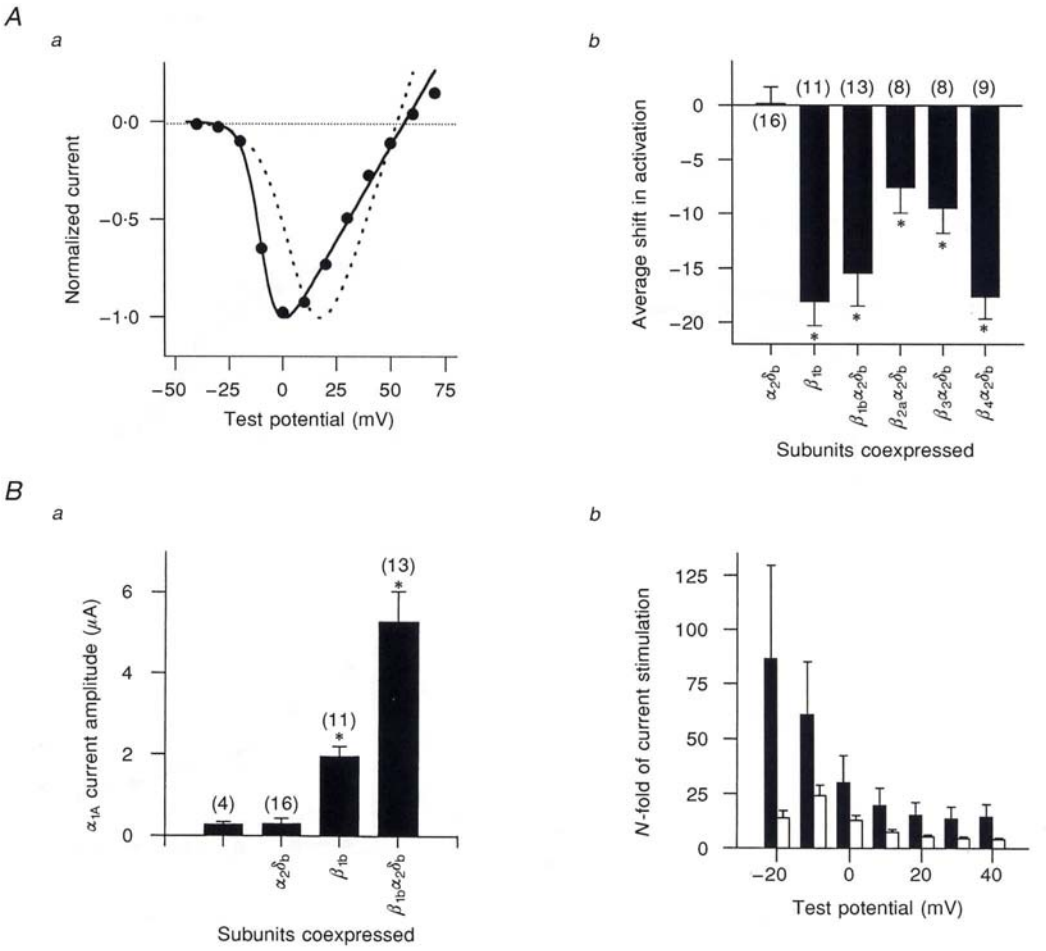

Figure 2. Regulation of α_{1A} currents by four β subunits and modulation by $\alpha_2\delta_b$ subunit
A, β_{1b} subunits shift the current–voltage relationship towards hyperpolarized potentials. *Aa*, normalized mean current–voltage relationship for α_{1A} (dashed line, same data as Fig. 1*A*) and $\alpha_{1A}\beta_{1b}$ (n = 11, ●, continuous line). Fit of the activation data yields g = 39·1 μS, E= 56 mV, $V_{½}$ = –9·9 mV and k = 4·2 mV for $\alpha_{1A}\beta_{1b}$, currents. The peak current amplitudes and the curve generated by the fit were normalized to the maximal current amplitude reached during the protocol of activation. *Ab*, mean hyperpolarizing shifts in current–voltage relationship by $\alpha_2\delta_b$ (same data as in Fig. 1*A*) and by various $\alpha_2\delta_b\beta$ subunit combinations. Fits to the mean activation data yield g = 105·6 ($\alpha_{1A}\alpha_2\delta_b\beta_{1b}$, n = 13), 35·1 ($\alpha_{1A}\alpha_2\delta_b\beta_{2a}$, n = 8), 34·8 ($\alpha_{1A}\alpha_2\delta_b\beta_3$, n = 8) and 106 μS ($\alpha_{1A}\alpha_2\delta_b\beta_4$, n = 9); E = 60·7 ($\alpha_{1A}\alpha_2\delta_b\beta_{1b}$ and $\alpha_{1A}\alpha_2\delta_b\beta_{2a}$) and 59·4 mV ($\alpha_{1A}\alpha_2\delta_b\beta_3$ and $\alpha_{1A}\alpha_2\delta_b\beta_4$); $V_{½}$ = –6·2 ($\alpha_{1A}\alpha_2\delta_b\beta_{1b}$), –5·7 ($\alpha_{1A}\alpha_2\delta_b\beta_{2a}$), 1·9 ($\alpha_{1A}\alpha_2\delta_b\beta_3$) and –9·8 mV ($\alpha_{1A}\alpha_2\delta_b\beta_4$); and k = 6·5 ($\alpha_{1A}\alpha_2\delta_b\beta_{1b}$), 5·3 ($\alpha_{1A}\alpha_2\delta_b\beta_{2a}$), 5·1 ($\alpha_{1A}\alpha_2\delta_b\beta_3$) and 3·8 mV ($\alpha_{1A}\alpha_2\delta_b\beta_4$). *B*, the current amplitude stimulation by ancillary subunits is more pronounced at hyperpolarized potentials. *Ba*, maximum current amplitude of the α_{1A} Ca^{2+} channel in various subunit combinations. *Bb*, α_{1A} current amplitude stimulation provided by the expression of α_{1b} subunit with (■) or without (□) the coexpression of $\alpha_2\delta_b$ subunit as a function of depolarization. Number of oocytes studied are n = 4 (α_{1A}), n = 16 ($\alpha_{1A}\alpha_2\delta_b$), n = 11 ($\alpha_{1A}\beta_{1b}$) and n = 13 ($\alpha_{1A}\alpha_2\delta_b\beta_{1b}$).

similar reduction in stimulation efficiency was also observed with stronger depolarizations in the absence of the $\alpha_{2}\delta_{b}$ subunit.

The voltage dependence of inactivation of the α_{1A} Ca^{2+} channel was also shifted towards more negative potentials by the association of β subunits. At a holding potential of –55 mV more than 50% of the $\alpha_{1A}\beta_{1b}$ channels were inactivated, whereas only a small fraction of α_{1A} channels were inactivated at a similar potential (compare Fig. 3*Aa* with Fig. 1*B*).

$\alpha_{1A}\beta_{1b}$ Ca^{2+} channels had a mean mid-point of inactivation of –61·2 ± 1·2 mV (n = 9) which, compared with –46 mV for the α_{1A} Ca^{2+} channel, corresponded to a hyperpolarizing shift of 15 ± 2mV (Fig.3*A*). Expression of the $\alpha_{2}\delta_{b}$ subunit did not modify the direction and amplitude of the β-induced shift in inactivation (Fig. 3*B*). Overall, the expression of β_{1b} submit resulted in a 17 ± 4 mV shift from a mid-point of inactivation of –42 ($\alpha_{1A}\alpha_{2}\delta_{b}$) to –59·5 ± 2·8 mV ($n$ = 13, $\alpha_{1A}\alpha_{2}\delta_{b}\beta_{1b}$). These shifts in steady-state inactivation were observed for all four β subunits with mid-points of inactivation of –56·6 ± 2 mV for β_{2a} (n = 7), –58·6 ±1·9 mV for β_{3} (n = 6) and –65·5 ± 1·3 mV for β_{4} (n = 7). Again, the β subunits could be classified according to their ability to shift the voltage dependence of inactivation with $\beta_{4} > \beta_{1b} = \beta_{3} = \beta_{2a}$.

The inactivation kinetics of the α_{1A} Ca^{2+} channel were also modified by the β subunits or by $\alpha_{2}\delta_{b}$–β subunit combinations. For all four β subunits studied, the kinetics of α_{1A} Ca^{2+} channel currents were converted from a biexponential to a monoexponential decay (Fig. 4).

In marked contrast with the biexponential decay of the α_{1A} subunit, $\alpha_{1A}\beta_{1b}$ Ca^{2+} channels inactivated along a single

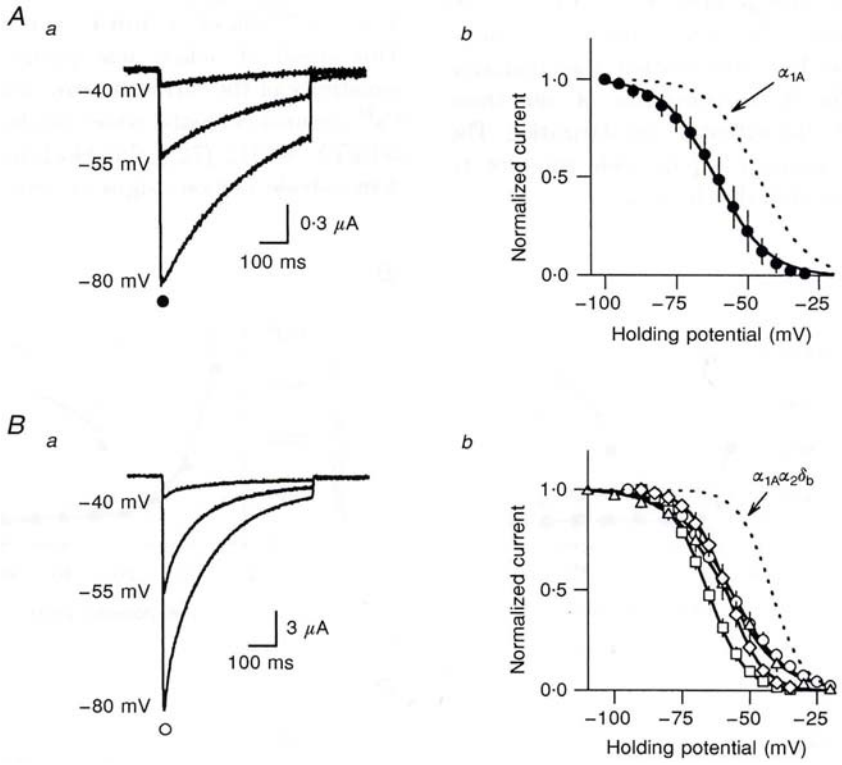

Figure 3. β subunits regulate the voltage dependence of inactivation
A, the β_{1b} subunit shifted the steady-state inactivation curve towards hyperpolarized potentials. *Aa*, trace examples of $\alpha_{1A}\beta_{1b}$ Ca^{2+} channel inactivation at –80, –55 and –40 mV holding potentials. Test potential is 10 mV. *Ab*, normalized mean steady-state inactivation curve for α_{1A} currents (dashed line, same data as in Fig. 1*B*) and $\alpha_{1A}\beta_{1b}$ currents (●, continuous line). Fit to the mean $\alpha_{1A}\beta_{1b}$ data yields $V_{½}$ = –61·3 mV and k = 9 mV for $\alpha_{1A}\beta_{1b}$ currents (n = 9). *B*, all β subunits induced similar shifts in the voltage dependence of inactivation. The amplitudes of these shifts were not modified by the $\alpha_{2}\delta_{b}$ subunit. *Ba*, trace examples of $\alpha_{1A}\alpha_{2}\delta_{b}\beta_{1b}$ current at holding potentials of –90, –55 and –40 mV to show steady-state inactivation. Test potential was 10 mV. *Bb*, normalized mean steady-state inactivation curve for currents (dashed line, same data as in Fig. 1*B*) and $\alpha_{1A}\alpha_{2}\delta_{b}$ coexpressed with various β subunits (different symbols, continuous lines). Fitting parameters are $V_{½}$ = –58·9 (β_{1b}, n = 9), –57 (β_{2a}, n = 7), –58·6 (β_{3}, n = 6) and –65·6 mV (β_{4}, n = 8), and k = 10·5 (β_{1b}), 10·3 (β_{2a}), 6·7 (β_{3}) and 7 mV (β_{4}) for mean data. ○, +β_{1b}; △,+β_{2a}; ◇, +β_{3}; □, +β_{4}.

inactivating component with a time constant of 490 ± 27 ms at 10 mV (n = 11). At the same potential, the inactivation of the α_{1A} Ca^{2+} channel was characterized by two time constants of 31 ± 1 and 498 ± 39 ms (n = 4). Although the inactivation kinetics of the α_{1A} Ca^{2+} channel were not regulated by $\alpha_2\delta_b$ in the absence of β subunits, we found that expression of $\alpha_2\delta_b$ influenced the rate by which the current inactivated in the presence of β subunits. At 10 mV, the decay of $\alpha_{1A}\alpha_2\delta_b\beta_{1b}$ Ca^{2+} channel current occurred with a time constant, τ, of 211 ± 19 ms (n = 14). This is therefore 2·3 times faster than the decay of $\alpha_{1A}\beta_{1b}$ Ca^{2+} channels at the same potential. All four β subunits were equally able to induce a monoexponential decay of either α_{1A} or $\alpha_{1A}\alpha_2\delta_b$ Ca^{2+} channel currents. However the various β subunits induced different time constants of inactivation. For instance, we measured the following τ values for each β subunit at 30 mV: 214 ± 18 ms (n = 14) for $\alpha_{1A}\alpha_2\delta_b\beta_{1b}$, 533 ± 28ms ($n$ = 8) for $\alpha_{1A}\alpha_2\delta_b\beta_{2a}$, 127 ± 6 ms ($n$ = 8) for $\alpha_{1A}\alpha_2\delta_b\beta_3$ and 243 ± 24 ms (n = 8) for $\alpha_{1A}\alpha_2\delta_b\beta_4$ Ca^{2+} channels. The rank order of β subunits with respect to the speed of inactivation was therefore $\beta_3 > \beta_{1b} = \beta_4 > \beta_{2a}$. The time constants of all these channels were sensitive to the extent of depolarization. The time constants were minimal for potentials superior to 0 mV that maximally activated the channels.

Ancillary subunits affect the rate of run-down but not the toxin sensitivity of the α_{1A} Ca^{2+} channel

We have examined the effects of $\alpha_2\delta_b$ and β subunit expression on the potency of ω-CgTX MVIIC to inhibit Ca^{2+} channel currents by studying the blocking time course of the toxin (Fig. 5).

The recordings were performed in 2 mM extracellular Ba^{2+} since the potency of ω-CgTX MVIIC is inhibited by increases in divalent cation concentration (not shown). We found that the blocking time course of 2 μM ω-CgTX MVIIC apparently differed slightly depending on the subunit composition. In all cases, the block of Ba^{2+} currents at this toxin concentration would have been completed if followed out to their steady-state values. Control experiments showed that the differences in blocking time course were mostly due to differences in rate of run-down of the various Ca^{2+} channel complexes. The block of $\alpha_{1A}\alpha_2\delta_b\beta_{1b}$ Ca^{2+} channel current was fast with a 97·8 + 0·7% block within 10 min of the toxin application. This speed of action was partly due to the increased sensitivity of the current to run-down. In contrast, $\alpha_{1A}\alpha_2\delta_b$ Ca^{2+} channel currents, which are less efficiently blocked by ω-CgTX MVIIC (72 ± 7% block in 10 min), also failed to demonstrate obvious signs of run-down. However, slight

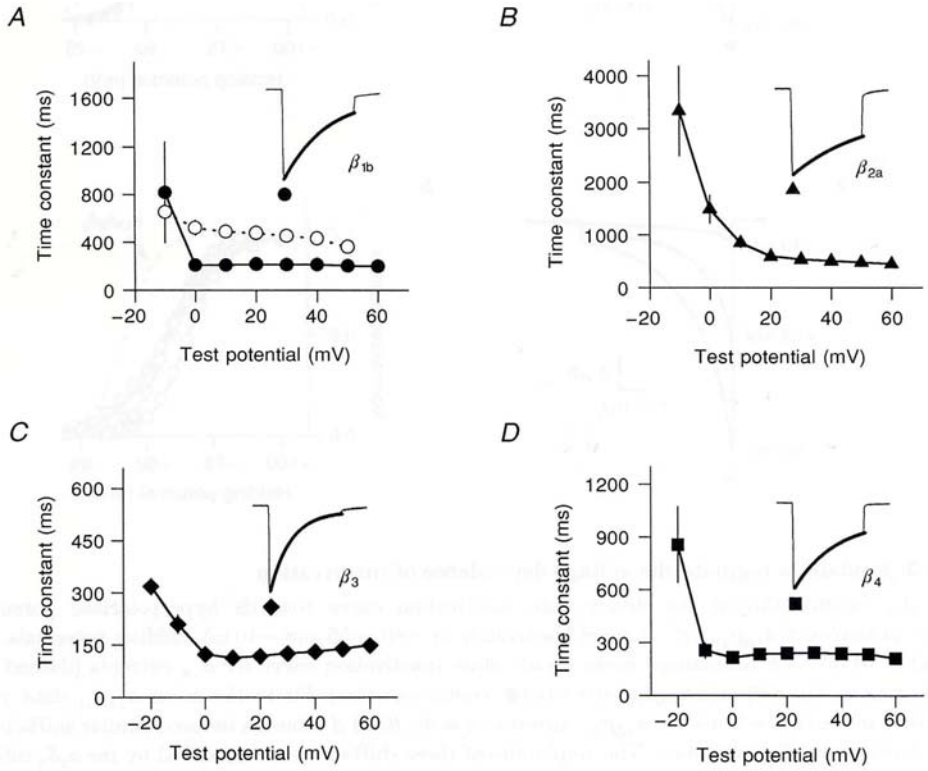

Figure 4. β subunits differentially regulate the inactivation kinetics of α_{1A} currents

A, mean time constants of α_{1A} current inactivation upon coexpression of β_{1b}, subunit with (●, continuous line, n= 14) or without $\alpha_2\delta_b$ (○, dashed line, n = 11) as a function of test potential. Inset, example of $\alpha_{1A}\alpha_2\delta_b\beta_{1b}$ current at 30 mV and monoexponential fit to the inactivating current (thick line). *B*, *C* and *D*, same as in *A* for $\alpha_{1A}\alpha_2\delta_b\beta_{2a}$ (▲, n = 8), $\alpha_{1A}\alpha_2\delta_b\beta_3$ (◆, n = 8) and $\alpha_{1A}\alpha_2\delta_b\beta_4$ (■, n = 9), respectively.

contributions of both $\alpha_2\delta_b$ and β subunits to the toxin sensitivity cannot be ruled out since run-down did not account for all the observed changes in the blocking effect of the toxin. For instance, a 10 min application of ω-CgTX MVIIC resulted in a 98% block of $\alpha_{1A}\alpha_2\delta_b\beta_{1b}$ current and a lower 81·3 ± 3·2% block of $\alpha_{1A}\beta_{1b}$ current, despite respective run-down values of 39·6 ± 9·8 and 57·3 ± 4·1 % suggesting a facilitatory action of $\alpha_2\delta_b$ on the toxin block. Overall, our data suggest that inhibitory mechanisms, responsible for the decrease of channel activity during run-down, may be acting on β subunits. The fact that β subunits are required for high functional expression of voltage-dependent Ca^{2+} channels is consistent with this observation. The data also demonstrate that α_{1A} is the only receptor for ω-GgTX MVIIC and that β and $\alpha_2\delta_b$ subunits may slightly regulate the blocking properties of this toxin at 2 μM in accordance with the important changes in the biophysical properties of the current.

The α_{1A} Ca^{2+} channel can be activated by weak depolarizations if the recordings are performed with low divalent cation concentrations

It has recently been suggested that the α_{1E} subunit is a low-voltage-activated channel (Soong *et al.* 1993). However, the voltage dependence of this Ca^{2+} channel has been recorded with low divalent cation concentrations as a source of permeant ion. By screening negative charges at the surface of the plasma membrane, changes in divalent cation concentrations are known to affect the transmembrane potential sensed by a Ca^{2+} channel. Therefore, accurate comparison of the voltage dependence of various cloned α_1 subunits has been made difficult by the experimental use of different extracellular Ba^{2+} concentrations. In order to normalize for the experimental conditions, we examined to what extent the peak of the current–voltage relationship could be modified by changes in divalent cation concentrations. Figure 6 reports the normalized peak current of the $\alpha_{1A}\alpha_2\delta_b\beta_{1b}$ Ca^{2+} channel in various Ba^{2+} concentrations. We found that very significant current amplitudes could be recorded despite large reductions in the extracellular Ba^{2+} concentration. The current amplitude was maximal at 40 mM Ba^{2+}. Reductions in current amplitude occurred at concentrations below 30 mM, and the estimated half-current amplitude occurred around 3 mM Ba^{2+}.

As expected, the reduction in the extracellular Ba^{2+} concentration resulted in hyperpolarizing shifts of the current–voltage relationship of activation (Fig. 7). At 2 mM Ba^{2+}, for instance, the peak current was reached at –23 mV which can be directly compared with a peak at

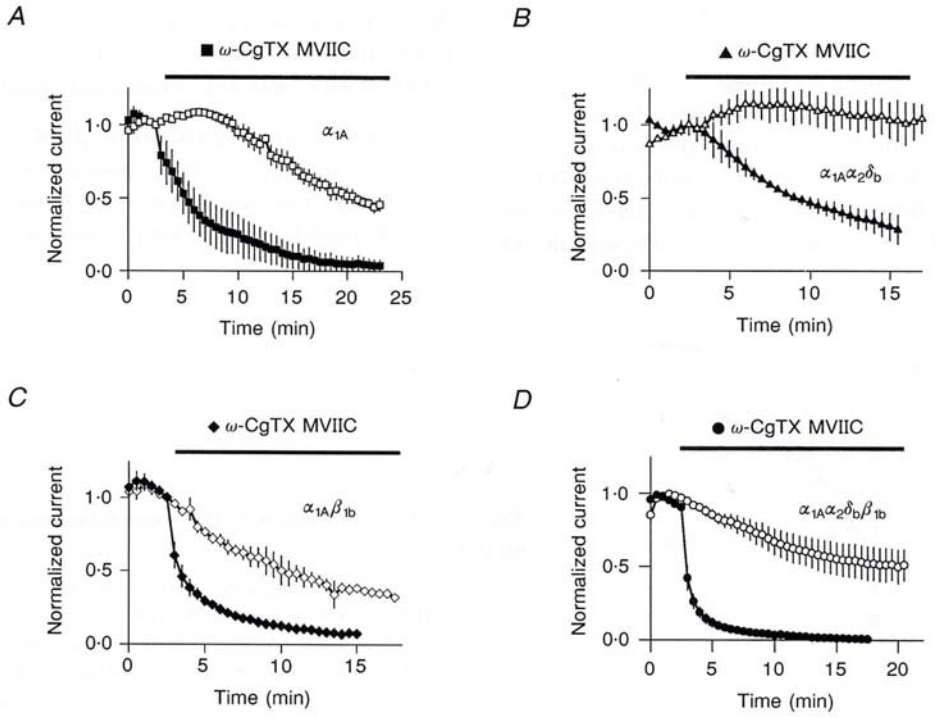

Figure 5. Effects of β and $\alpha_2\delta_b$ subunits on the rate of run-down and rate of ω-CgTX MVIIC block

A, average rate of run-down of α_{1A} currents (open symbols, n = 4) and mean rate of current block by 2 μM ω-CgTX MVIIC (filled symbols, n = 4). External Ba^{2+} concentration was 2 mM, holding potential –90 mV and test potential –10 mV. The cells were stimulated every 30 s. The current amplitude of each pulse was normalized to the last control current amplitude prior to application of the toxin. *B*, *C* and *D*, same experiments as in *A* for $\alpha_{1A}\alpha_2\delta_b$ (n = 6), $\alpha_{1A}\beta_{1b}$ (n = 6) and $\alpha_{1A}\alpha_2\delta_b\beta_{1b}$ (n = 10) currents, respectively.

6 mV in 40 mM Ba^{2+}. Thus, reducing the permeant cation to near physiological concentrations was enough to provoke a hyperpolarizing shift of 29 mV. We estimated that at 4 mM Ba^{2+}, the peak current occurs at a potential of –14·2 mV which is comparable to a potential of –10 mV for α_{1E} currents under similar experimental conditions (Soong *et al.* 1993).

We conclude, therefore, that α_{1A} cannot be distinguished by its voltage dependence from the α_{1E} subunit and that, contrary to an initial report (Mori et al. 1991), the α_{1A} subunit is also more likely to behave as a low-voltage-activated channel in a more physiological divalent cation concentration.

DISCUSSION

The α_{1A} subunit alone is sufficient to direct the expression of functional Ca^{2+} channels

The low level of expression of the α_{1A} Ca^{2+} channel in the absence of β subunits has been a serious limitation to its functional characterization (Mori *et al.* 1991). Also, because so little expression could be observed in the absence of auxiliary subunits, their effects on the functional properties of the α_{1A} subunit have not been qualitatively and quantitatively well assessed. Our data demonstrate for the first time that α_{1A} Ca^{2+} channels can give rise to significant levels of expression on their own. The α_{1A} subunit carries the main properties of this neuronal Ca^{2+} channel, such as ionic permeability, gating, voltage sensitivity and pharmacology. Probably the most striking observation is that RNA coding for this subunit causes the appearance of Ba^{2+} current that displays not one, but two kinetic components. Since these two components have similar pharmacological and biophysical properties, we can rule out the possibility that they both originate from two distinct Ca^{2+} channel conductances. Instead, the data suggest that a single α_1 molecule can display a complex macroscopic behaviour. It also remains possible that differential processing and modulation of a fraction of these molecules favours the appearance of a population of channels with different functional properties. In the study presented here, a better description of the properties of α_{1A} Ca^{2+} channels in the absence of auxiliary subunits has been a key determinant in the understanding of the regulatory contribution of these auxiliary subunits themselves. Our findings illustrate that two of the ancillary subunits ($\alpha_2\delta$ and β), which are the most likely to associate with α_{1A} directly interact with the channel and regulate the current activities in specific ways. We analysed the differences in current properties introduced by β, $\alpha_2\delta_b$ or a combination of both subunit types and used these differences as an index of the functional contribution of each of these auxiliary subunits.

Auxiliary β subunits of voltage-gated Ca^{2+} channels regulate the properties of the α_{1A} subunit: implications for the underlying molecular mechanisms.

Of the two subunits that are the most likely to assemble with the α_{1A} subunit *in vivo*, β subunits have the most dramatic regulatory properties. We report four primary functional modifications that are well conserved among β subunits with, however, some minor quantitative differences.

The most obvious regulation by β subunits is the dramatic increase in α_{1A} current amplitude. The mechanism underlying this stimulation is best understood for the α_{1C} Ca^{2+} channel for which comparable data are available. The

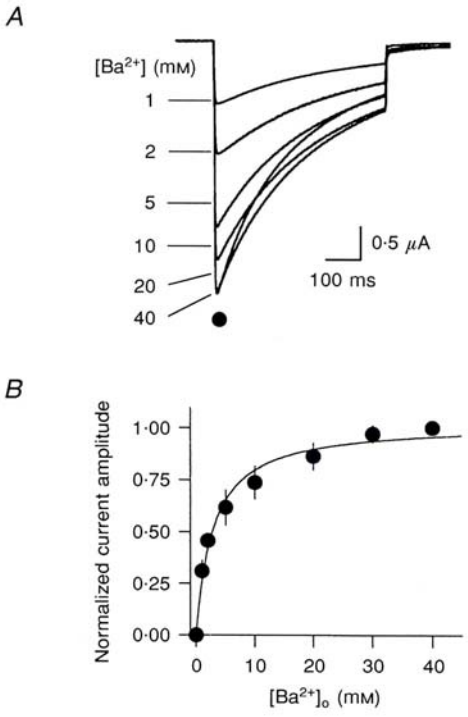

Figure 6. Relation between Ba^{2+} concentration and current amplitude

A, trace examples of $\alpha_{1A}\alpha_2\delta_b\beta_{1b}$ currents in various Ba^{2+} concentrations. Traces represent the peak of current–voltage relationship at each Ba^{2+} concentration. *B*, mean current increase as a function of the extracellular Ba^{2+} concentration ($[Ba^{2+}]_0$). Current amplitudes were normalized to the peak current obtained at 40 mM Ba^{2+}. The data represent the mean of $n = 4$ experiments (± S.E.M.). The data are fitted with a hyperbolic function $I_{Ba} = I_{max}\,[Ba^{2+}]/([Ba^{2+}]_{½} + [Ba^{2+}])$, where I_{Ba} is the mean normalized current amplitude, I_{max} maximum normalized current ($I_{max} = 1{\cdot}025$), $[Ba^{2+}]$ the external Ba^{2+} concentration and $[Ba^{2+}]_{½}$ the Ba^{2+} concentration responsible for half-maximal current amplitude ($[Ba^{2+}]_{½} = 2{\cdot}9$ mM).

cardiac α_{1C} subunit is also the only channel for which a direct comparison between current density and dihydropyridine binding sites was reported. It was demonstrated that the increase in current triggered by β subunits can be correlated with an increase in the number of dihydropyridine binding sites (Perez-Reyes *et al.* 1992; Castellano *et al.* 1993*b*). Since dihydropyridines bind on the α_{1C} subunit, the increase both in the current and in the number of dihydropyridine binding sites would suggest that β subunits act by increasing the number of channels present at the plasma membrane. However, gating charge measurements (Neely, Wei, Olcese, Birnbaumer & Stefani, 1993) and immunoblot analysis (Nishimura, Takeshima, Hofmann, Flockerzi & Imoto, 1993) demonstrated instead that the number of α_{1C} submits expressed at the plasma membrane was in fact not altered by the β subunits. To reconcile what appear to be contradictory results, it was hypothesized that β subunits act primarily by inducing important conformational changes in the pore-forming subunit. These changes in α_1 subunit conformation would then in turn be responsible for an increase not only in the opening probability of the channel, but also in the accessibility of the drug to its site. Although no binding data are available for the α_{1A} subunit, our data suggest that

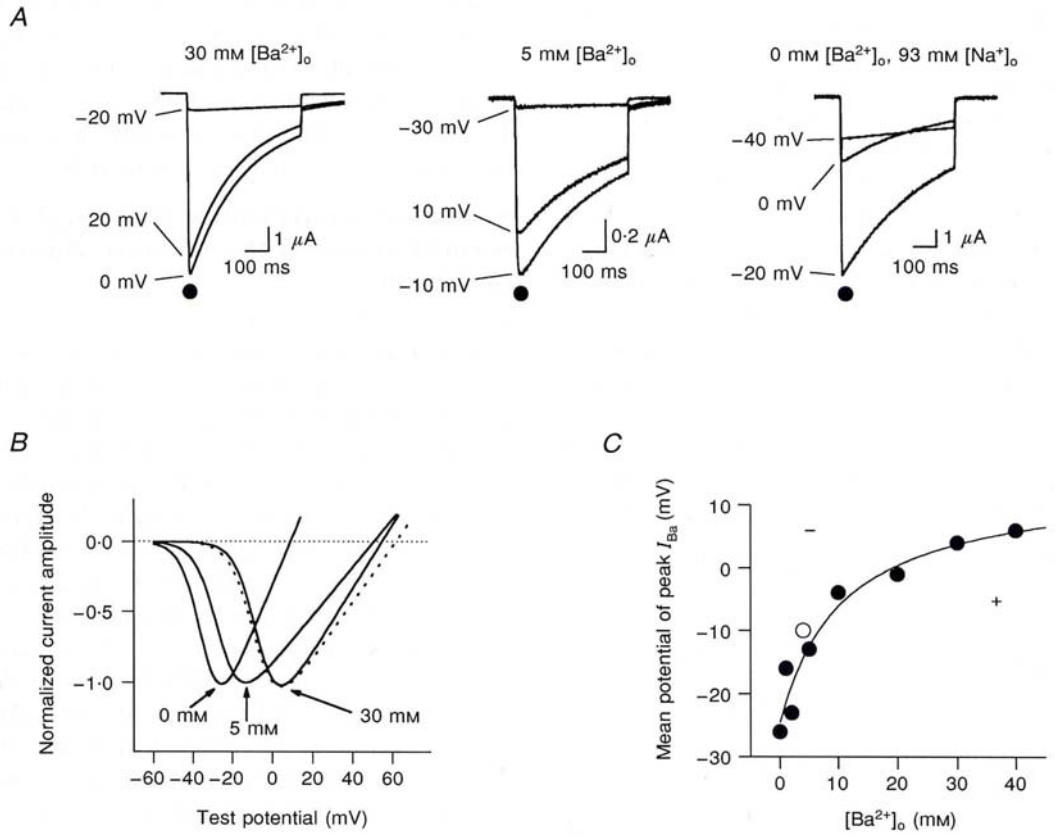

Figure 7. The current–voltage relationship of $\alpha_{1A}\alpha_2\delta_b\beta_{1b}$ currents is a function of the extracellular divalent cation concentration

A, trace examples of $\alpha_{1A}\alpha_2\delta_b\beta_{1b}$ currents with 30 and 5 mM Ba^{2+} and 0 mM Ba^+, 93 mM Na^+ in the extracellular solution. In 0 mM Ba^{2+}, extracellular Na^+ and intracellular K^+ were the charge carriers. With decreasing Ba^{2+} concentrations, the osmolarity of the solution was kept constant by adjusting the NaOH concentration (Table 1). *B*, average normalized current–voltage relationship for oocytes injected with $\alpha_{1A}\alpha_2\delta_b\beta_{1b}$ 30 (n = 6), 5 (n = 2) and 0 mM (n = 3, 93 mM Na^+) extracellular Ba^{2+} (continuous lines). The dashed line represents the current–voltage relation in 40 mM Ba^{2+}. Fit of the activation data yields g = 94, 68·6 and 130 μS, E=55, 50·5 and 9 mV, $V_{½}$ = –7, –27 and –35 mV, and k= 5·3, 5·7 and 5·1 mV for 30, 5 and 0 mV Ba^{2+}, respectively Note the hyperpolarizing shift in reversal potential when Na^+ and K^+ are the charge carriers. *C*, mean potential of peak current as a function of the extracellular Ba^{2+} concentration (n = 37 oocytes studied in total). The data were best described with a hyperbolic function: $V_{peak} = \{(V_{max}\ [Ba^{2+}]) / ([Ba^{2+}]_{½} + [Ba^{2+}])\} + V_0$ where a V_{max} of 38·7 mV was the maximum shift in peak potential induced by Ba^{2+}, $[Ba^{2+}]_{½}$ of 11·1 mM was the Ba^{2+} concentration that induced a half-maximal shift in peak potential, and V_0 of –24·5 mV was the peak potential of $\alpha_{1A}\alpha_2\delta_b\beta_{1b}$ in the absence of Ba^{2+}. Any point above this curve has a lower (–) voltage sensitivity than the α_{1A} channel. The open circle represents the potential of the peak current of the α_{1E} subunit at 4 mM Ba^{2+} (data from Soong *et al.* 1993).

the blocking potency, and therefore probably the affinity of ω-CgTX MVIIC for its binding site on this structurally related subunit, is only slightly modified by the expression of ancillary subunits. These findings suggest that the binding site to this toxin is not greatly affected by the β-induced conformational changes in the α_{1A} subunit. These observations are also consistent with the fact that ω-CgTX MVIIC binds to a different region on the α_1 molecule from the dihydropyridines.

All β subunits trigger significant changes in the voltage dependence of the α_{1A} Ca^{2+} channel. The voltage dependence of both activation and inactivation are affected. The amplitude of the changes observed were either very similar among β subunits (inactivation) or differed slightly (activation). Since for all β subunits these shifts were directed towards more negative potentials, the molecular contribution of these subunits should be very similar. The functional equivalence between these subunits is, however, not complete if one considers the regulation of the inactivation kinetics. The β_{2a} subunit induces a very slow inactivation of the current whereas the β_3 subunit induces the fastest inactivation kinetics. Interestingly, although the various β subunits differ in their regulation of the time constant of inactivation, there is not a strong difference in the amplitude of the hyperpolarizing shift of the voltage-dependent inactivation process. These observations strongly suggest that the control of the inactivation kinetics and of the voltage dependence of inactivation of Ca^{2+} channels occurs by different mechanisms and molecular interactions.

Which β subunit is normally associated with the α_{1A} Ca^{2+} channel in neurons?

Because all β subunits seem to be capable of normalizing the properties of α_{1A}, it is difficult to infer from expression experiments which β subunit associates with this neuronal Ca^{2+} channel *in situ*. Our observations suggest, however, that the β_4 subunit has the most prominent effects on the properties of this channel. Firstly, our findings show that for most regulation, β subunits differ in the amplitude of their effects such that generally $\beta_4 \geqslant \beta_{1b} > \beta_3 = \beta_{2a}$ (Table 2). Since expression of the β_4 subunit induces the greatest shift in current amplitude and also the most significant shift in voltage dependence of inactivation, β_4 is the most likely β subunit associated with α_{1A}. Secondly, both α_{1A} and β_4 subunits have been found to be highly expressed in the cerebellum, as assessed by 'Northern blot' analysis (Starr, Prystay & Snutch, 1991; Castellano *et al.* 1993*b*) increasing the likelihood of their association *in vivo*.

Although β subunits contribute to a larger calcium influx, they also impart to the channel an increased sensitivity to cell inhibitory regulation

Our data show that the increase in current amplitude and the hyperpolarizing shift in activation would both account for an increase in calcium influx. However, since these two primary regulations do not occur independently of each other, the stimulation of Ca^{2+} current by β subunits is even more dramatic. This is particularly true at hyperpolarized potentials where β subunits would dramatically increase the amount of Ca^{2+} influx during an action potential. A consequence of the stimulatory function of β subunits is also an increased need for inhibitory cellular mechanisms capable of controlling the Ca^{2+} influx into the cell. Remarkably, cell inhibitory mechanisms can be favoured by two additional modes of β subunit regulation. For instance, the hyperpolarizing shift in the voltage dependence of steady-state inactivation should clearly increase the sensitivity of the channel to inactivation by cell depolarization. Such a mechanism would represent a simple and efficient mechanism of calcium entry limitation. Also, by a process that is still not well understood, we found that β subunits increase the sensitivity of Ca^{2+} channels to run-down. Of course, run-down represents a more definitive cell inhibitory mechanism of the channel activity.

Association of β subunits with the α_{1A} Ca^{2+} channel is essential to uncover the functional importance of the $\alpha_2\delta$ subunit

None of the four biophysical properties of the α_{1A} Ca^{2+} channel studied were modified by $\alpha_2\delta$ in the absence of β subunits. Although RNA coding for an endogenous $\alpha_2\delta$ subunit has been detected in oocytes (Singer-Lahat, Lotan, Itagaki, Schwartz & Dascal, 1992), it is unlikely that the $\alpha_2\delta$ protein is present in sufficient amounts to associate with the α_{1A} subunit. Although the presence of an endogenous $\alpha_2\delta$ could have explained the observed lack of regulation of the α_{1A} channel by the exogenous $\alpha_2\delta$ subunit, this possibility is remote because (1) native oocytes show only low levels of endogenous Ca^{2+} channel activity and (2) injection of exogenous $\alpha_2\delta$ cRNA enhances the expression of exogenous α_{1C} cRNA (Singer *et al.* 1991). Also, we found that the exogenous $\alpha_2\delta_b$ subunit modulates the β-induced Ca^{2+} current stimulation and inactivation kinetics changes. Interaction sites of $\alpha_2\delta$ subunits have not been mapped yet in Ca^{2+}channels. However, despite the fact that the functional contributions of $\alpha_2\delta$ in the presence of β subunits (current amplitude stimulation and change in inactivation kinetics) are of the same nature as those induced by β subunits alone, direct $\alpha_2\delta$–β interactions are unlikely to explain the data. It has been shown that β subunits are entirely cytoplasmic and the membrane topology of $\alpha_2\delta$ predicts that despite some hydrophobic segments this subunit is mostly extracellular (Jay, Sharp, Kahl, Vedvick, Harpold & Campbell, 1991). Instead, it seems more likely that the $\alpha_2\delta$ subunit is unable to interact with α_{1A} unless $\alpha_1 - \beta$ interactions have first occurred (Pragnell *et al.* 1994). This suggests that α_1–β subunit interactions could favour the occurrence of α_1–$\alpha_2\delta$ interactions via the same conformational changes that are required for enhanced current amplitude (Neely *et al.* 1993). In the presence of β

Table 2. Comparison of the functional effects of $\alpha_2\delta_b$ and β subunits on the properties of two cloned α_1 subunits

Properties analysed	α_{1A} subunit	α_{1C} subunit
Peak current increase by β	Between 5- and 19-fold with $\beta_4 = \beta_{1b} > \beta_3 = \beta_{2a}$	Between 3·5- and 11-fold by β_{1a}, β_2, β_3, and β_4[a–d]
Peak current increase by $\alpha_2\delta$	No increase in the absence of β subunit	Slight increase in the absence of β subunit (5)
	× 2·5 potentiation of the β subunit stimulation	Higher increase in the presence of β subunit
Change in activation kinetics by β or $\alpha_2\delta$	Not affected by β or $\alpha_2\delta_b$ subunits	Acceleration with $\beta_{2b} > \beta_{2a} > \beta_3 > \beta_{1a}$ n.a. for $\alpha_2\delta$[a–c]
Change in inactivation kinetics by β subunits	Monophasic decay with fastest rates $\beta_3 > \beta_{1b} = \beta_4 > \beta_{2a}$	Change by β_{1b}, β_2, β_3 and β_4 with $\beta_4 > \beta_3 > \beta_2$[a–c]
Change in inactivation kinetics by $\alpha_2\delta$	No change in the absence of β subunits	n.a.
	Increased inactivation in the presence of β subunits	n.a.
Change in voltage dependence of activation by β or $\alpha_2\delta$	Between –7 and –16 mV with $\beta_4 = \beta_{1b} > \beta_3 = \beta_{2a}$	Hyperpolarizing shift by β_{1a}, β_{1b}, β_2, β_3 and β_4
	Not modified by $\alpha_2\delta_b$	n.a. for $\alpha_2\delta$[a–d]
Change in voltage dependence of inactivation by β or $\alpha_2\delta$	Between –15 and –23 mV with $\beta_4 > \beta_{1b} = \beta_3 = \beta_{2a}$	No hyperpolarizing shift by β_{1b}, β_3 or β_4[b, c, f]
	Not modified by $\alpha_2\delta_b$	n.a.
Regulation of drug potency by β or $\alpha_2\delta$	Effect of ω–CgTX MVIIC modified by $\alpha_2\delta_b$ or β_{1b}	Bay K 8644 stimulation or nifedipine inhibition not affected by β_3, β_4 or $\alpha_2\delta_b$[b, c, f]
Increase in number of drug binding sites by β or $\alpha_2\delta$	n.a.	Increased number of dihydro–pyridine binding sites by β_2 and β_4[a, b]
Change in drug affinity by β or $\alpha_2\delta$	n.a.	Not modified by β subunits (β_2)[a]

[a] Perez-Beyes *et al.* 1992; [b] Castellano *et al.* 1993*b*; [c] Tomlinson *et al.* 1993; [d] Wei *et al.* 1991; [e] Mikami *et al.* 1989; [f] Castellano *et al.* 1993*a*; n.a., not applicable.

subunits, these α_1-$\alpha_2\delta$ interactions could in turn either directly regulate the α_{1A} properties or indirectly influence the regulatory contribution of β subunits.

Do auxilliary subunits regulate the same set of properties in all α_1 subunits?

We have underlined the functional similarities of all β subunits by demonstrating that they were able to shift the voltage dependence of activation and inactivation, to stimulate the current amplitude and to induce a monoexponential decay of the inactivation kinetics. We have also demonstrated that the increase in current and the changes in inactivation kinetics are also modulated by the $\alpha_2\delta$ subunit. To get some insights into the possible molecular mechanisms underlying subunit regulation in Ca^{2+} channels, we have examined the type and extent of regulation previously observed with structurally unrelated α_1 subunits. A very striking observation is that the subunit regulation processes observed with the α_{1A} Ca^{2+} channel have also been described for different α_1 Ca^{2+} channels. The stimulation in current amplitude by β subunits and the potentiation by the $\alpha_2\delta$ subunit have been observed for all α_1 subunits (Mori *et al.* 1991; Hullin *et al.* 1992; Williams *et al.* 1992*a*,*b*; Ellinor *et al.* 1993) with the exception of the α_{1E} subunit (Soong *et al.* 1993). Table 2 summarizes and compares both $\alpha_2\delta$ and β subunit regulation of two functionally and structurally different α_1 subunits. As for the α_{1A} Ca^{2+} channel, β subunits also increase the current amplitude, shift the voltage dependence of activation towards hyperpolarized potentials and modify the inactivation kinetics of the α_{1C} Ca^{2+} channel. It is interesting to observe that the order in which β subunits are classified, with respect to the rate constant of inactivation, is identical for α_{1A}, α_{1C} (Table 2) and Doe-1 Ca^{2+} channels (Ellinor *et al.* 1993). Also similar to events in the α_{1A} channel, β subunits shift the steady-state inactivation of α_{1B} Ca^{2+} channels 20 mV towards more negative potentials (Stea *et al.* 1993). Altogether, these results suggest that the regulation of the functional properties of various α_1 Ca^{2+} channels by β subunits occurs via a set of conserved interaction sites. These α_1–β interaction sites should also have identical functional consequences. One such interaction site has recently been reported with the identification of an amino acid motif that is present on the cytoplasmic linker between repeat I and II of every α_1 subunits. This repeat is essential to the current stimulation, the changes in voltage dependence and the modulation of inactivation kinetics (Pragnell *et al.* 1994). There is evidence to believe that, besides this primary interaction, additional sites may exist between these two subunits. The fact that β subunits do not regulate all α_1 subunits in a similar manner is consistent with this interpretation, β subunits do not shift the voltage dependence of steady-state inactivation of the α_{1C} subunit, nor affect the voltage dependence of activation of α_{1B} Ca^{2+} channels (Stea *et al.* 1993). Neither do they affect the activation kinetics of the α_{1A} channel. These observations appear to suggest that the mere existence of secondary α_1–β interaction sites is determined by the primary sequence of each α_1 subunit. The near complete functional equivalence of β subunits stands in contradiction with the apparent specificity of α_1–β interactions that has clearly been illustrated in two purified voltage-gated Ca^{2+} channels. Indeed, it remains to be understood why the α_{1B} subunit of the N-type Ca^{2+} channel or the α_{1S} subunit of the skeletal muscle dihydropyridine receptor, associate with the β_3 (Witcher *et al.* 1993) and the β_{1a} (Ruth *et al.* 1989) subunits, respectively.

Not all functional properties of native Ca^{2+} channels can be compared with properties of cloned Ca^{2+} channel subunits

With the increasing number of Ca^{2+} channel α_1 subunits being cloned, there is a natural propensity to correlate functionally these molecules to their native counterparts. Expression of the α_1 Ca^{2+} channel with various auxilliary subunits demonstrates the risks of interpretation involved in such an exercise. It is generally assumed that native Ca^{2+} channels are a complex of four subunits as illustrated by the subunit identification of the purified skeletal muscle L-type and neuronal N-type Ca^{2+} channels (Takahashi *et al.* 1987; Witcher *et al.* 1993). However, data about the subunit composition of other native Ca^{2+} channels are still lacking. Also, it cannot be ruled out that a significant fraction of each channel subtype may also exist as incomplete protein complexes in the plasma membrane (i.e. α_1, $\alpha_1\alpha_2\delta$, $\alpha_1\beta$ and $\alpha_1\alpha_2\delta\beta$ Ca^{2+} channels). Although this question will ultimately be resolved by a better knowledge of the cellular processing of Ca^{2+} channels, it raises the intriguing possibility that part of the biophysical variability of each native Ca^{2+} channel may also arise from a variability in their subunit composition. Besides differences in pharmacological properties, gating, permeability and voltage dependence of activation and inactivation have all been used as critical determinants for the biophysical classification of various Ca^{2+} channel subtypes (Bean, 1989). However, the expression data show, for example, that multiple inactivating components can be detected in the kinetics of α_{1A} or $\alpha_{1A}\alpha_2\delta$ Ca^{2+} channels despite the clear molecular homogeneity of these channel populations. These results demonstrate that the kinetics of inactivation cannot be used as a reliable criterion of Ca^{2+} channel identification. This is also further illustrated by the fact that the number and rate constants of the inactivating components are under the strict control of the associating subunits. Not only do the β subunits change the number of inactivating components from two to one, but they also differentially affect the rate constant of inactivation of the α_{1A} Ca^{2+} channel. Also, since different β subunits affect the voltage dependence of both activation and inactivation processes to various extents, these parameters do not represent ideal tools of channel identification and classification. Finally, much confusion has arisen concerning the voltage dependence of various cloned α_1 subunits. Our data demonstrate that despite the fact

that α_{1A} (Mori *et al.* 1991) and α_{1E} (Soong *et al.* 1993) subunits were initially classified as high- and low-voltage-activated Ca^{2+} channels, respectively, there are in reality no differences in the voltage sensitivity of these two channels. Overall expression data illustrate the risks involved in discriminating native Ca^{2+} channels by their biophysical properties. The findings also suggest that the functional comparison between the cloned α_{1A} subunit and the native P-type Ca^{2+} channel (Sather *et al.* 1993) should await the data on the purification and the subunit identification of this neuronal Ca^{2+} channel.

BEAN, B. P. (1989). Classes of calcium channels in vertebrate cells. *Annual Review of Physiology* **51**, 367–384.

BIRNBAUMER, L., CAMPBELL, K. P., CATTERALL, W. A., HARPOLD, M.M., HOFMANN, P., HORNE, W. A., MORI, Y., SCHWARTZ, A., SNUTCH, T. P., TANABE, T. & TSIEN, R. W. (1994). The naming of voltage-gated calcium channels. *Neuron* **13**, 505–506.

CASTELLANO, A., WEI, X., BIRNBAUMER, L. & PEREZ-REYES, E. (1993*a*). Cloning and expression of a third calcium channel β subunit. *Journal of Biological Chemistry* **268**, 3450–3455.

CASTELLANO, A., WEI, X., BIRNBAUMER, L. & PEREZ-REYES, E. (1993*b*). Cloning and expression of a neuronal calcium channel β subunit. *Journal of Biological Chemistry* **268**, 12359–12366.

DASCAL, N. (1987). The use of *Xenopus* oocytes for the study of ion channels. *CRC Critical Reviews in Biochemistry* **22**, 317–387.

DE WAARD, M., WITCHER, D. R. & CAMPBELL, K. P. (1994). Functional properties of the purified N-type Ca^{2+} channel from rabbit brain. *Journal of Biological Chemistry* **269**, 6716–6724.

DUBEL, S. J., STARK, T. V. B., HELL, J., AHLIJANIAN, M. K., ENYEART, J. J., CATTERALL, W. A. & SNUTCH, T. P. (1992). Molecular cloning of the *a*l subunit of an ω-conotoxin-sensitive calcium channel. *Proceedings of the National Academy of Sciences of the USA* **89**, 5058–5062.

ELLINOR, P. T., ZHANG, J.-F., RANDALL, A. D., ZHOU, M., SCHWARZ, T. L., TSIEN, R. W. & HORNE, W. A. (1993). Functional expression of a rapidly inactivating neuronal calcium channel. *Nature* **363**, 455–458.

ELLIS, S. B., WILLIAMS, M. E., WAYS, N. R., BRENNER, R., SHARP, A. H., LEUNG, A. T., CAMPBELL, K. P., MCKENNA, E., KOCH, W. J., HUI, A., SCHWARTZ, A. & HARPOLD, M. M. (1988). Sequence and expression of mRNAs encoding the α_1 and α_2 subunits of a DHP-sensitive calcium channel. *Science* **241**, 1661–1664.

EPPIG, J. J. & DUMONT, J. N. (1976). Defined nutrient medium for the *in vitro* maintenance of *Xenopus laevis* oocytes. *In Vitro* **12**, 418–427.

HILLYARD, D. R., MONJE, V. D., MINTZ, I. M., BEAN, B. P., NADASDI, L., RAMACHANDRAN, J., MILJANICH, G., AZIMI-ZOONOOZ, A., MCINTOSH, J. M., CRUZ, L. J., IMPERIAL, J. S. & OLIVERA, B. M. (1992). A new conus peptide ligand for mammalian presynaptic Ca^{2+} channels. *Neuron* **9**, 69–77.

HUI, A., ELLINOR, P. T, KRIZANOVA, O., WANG, J.-J., DIEBOLD, R. J. & SCHWARTZ, A. (1991). Molecular cloning of multiple subtypes of a novel rat brain isoform of the α_1 subunit of the voltage dependent calcium channel. *Neuron* **7**, 35–44.

HULIN, R., SINOER-LAHAT, D., FREICHEL, M., BIEL, M., DASCAL, N., HOFMANN, F. & FLOCKERZI, V. (1992). Calcium channel β subunit heterogeneity: functional expression of cloned cDNA from heart, aorta and brain. *EMBO Journal* **11**, 885–890.

JAY, S. D., ELLIS, S. B., MCCUE, A. F., WILLIAMS, M. E., VEDVICK, T.S., HARPOLD, M. M. & CAMPBELL, K. P. (1990). Primary structure of the γ subunit of the DHP-sensitive calcium channel from skeletal muscle. *Science* **248**, 490–492.

JAY, S. D., SHARP, A. H., KAHL, S. D., VEDVICK, T. S., HARPOLD, M. M. & CAMPBELL, K. P. (1991). Structural characterization of the dihydropyridine -sensitive calcium channel α_2-subunit and the associated δ peptides. *Journal of Biological Chemistry* **266**, 3287–3293.

KIM, H.-L., KIM, H., LEE, P., KING, R. & CHIN, H. (1992). Rat brain expresses an alternatively spliced form of the dihydropyridine-sensitive L-type calcium channel α_2 subunit. *Proceedings of the National Academy of Sciences of the USA* **89**, 3251–3255.

LACERDA, A. E., KIM, H. S., RUTH, P., PEREZ-REYES, E., FLOCKERZI, V., HOFMANN, F., BIRNBAUMER, L. & BROWN, A. M. (1991). Normalization of current kinetics by interaction between the α_1 and β subunits of the skeletal muscle dihydropyridine-sensitive Ca^{2+} channel. *Nature* **352**, 527–530.

MIKAMI, A., IMOTO, K., TANABE, T., NIIDOME, T., MORI, Y., TAKESHIMA, H., NARUMIYA, S. & NUMA, S. (1989). Primary structure and functional expression of the cardiac dihydropyridine-sensitive calcium channel. *Nature* **340**, 230–233.

MILLER, R. (1992). Voltage-sensitive Ca^{2+} channels. *Journal of Biological Chemistry* **267**, 1403–1406.

MORI, Y, FRIEDRICH, T., KIM, M.-S., MIKAMI, A., NAKAI, J., RUTH, P., BOSSE, E., HOFMANN, F, FLOCKERZI, V., FURUICHI, T., MIKOSHIBA, K., IMOTO, K., TANABE, T. & NUMA, S. (1991). Primary structure and functional expression from complementary DNA of a brain calcium channel. *Nature* **350**, 398–402.

MORTON, M. E. & FROEHNER, S. C. (1989). The α_1 and α_2 polypeptides of the dihydropyridine-sensitive calcium channel differ in developmental expression and tissue distribution. *Neuron* **2**, 1499–1506.

NEELY, A., WEI, X., OLCESE, R., BIRNBAUMER, L. & STEFANI, E. (1993). Potentiation by the β subunit of the ratio of the ionic current to the charge movement in the cardiac calcium channel. *Science* **262**, 575–578.

NIIDOME, T., KIM, M.-S., FRIEDRICH, T. & MORI, Y. (1992). Molecular cloning and characterization of a novel calcium channel from rabbit brain. *FEBS Letters* **308**, 7–13.

NISHIMURA, S., TAKESHIMA, H., HOFMANN, F, FLOCKERZI, V. & IMOTO, K. (1993). Requirement of the calcium channel β subunit for functional conformation. *FEBS Letters* **324**, 283–286.

PEREZ-REYES, E., CASTELLANO, A., KIM, H. S., BERTRAND, P., BAGGSTROM, E., LACERDA, A. E., WEI, X. & BIRNBAUMER, L. (1992). Cloning and expression of a cardiac/brain β subunit of the L-type calcium channel. *Journal of Biological Chemistry* **267**, 1792–1797.

PRAGNELL, M., DE WAARD, M., MORI, Y, TANABE, T, SNUTCH, T. P. & CAMPBELL, K. P. (1994). Calcium channel β-subunit binds to a conserved motif in the I-II cytoplasmic linker of the α_1-subunit. *Nature* **368**, 67-70.

PRAGNELL, M., SAKAMOTO, J., JAY, S. D. & CAMPBELL, K. P. (1991). Cloning and tissue specific expression of the brain calcium channel β-subunit. *FEBS Letters* **291**, 253–258.

RUTH, P., ROHRKAZTEN, A., BIEL, M., BOSSE, E., REGULLA, S., MEYER, H. E., FLOCKERZI, V. & HOFMANN, F. (1989). Primary structure of the β subunit of the DHP-sensitive calcium channel from skeletal muscle. *Science* **245**, 1115–1118.

SATHER, W. A., TANABE, T, ZHANG, J.-F., MORI, Y, ADAMS, M. E. & TSIEN, R. W. (1993). Distinctive biophysical and pharmacological properties of class A (BI) calcium channel α_1 subunits. *Neuron* **11**, 291–303.

SINGER, D., BIEL, M., LOTAN, I., FLOCKERZI, V., HOFMANN, F. & DASCAL, N. (1991). The roles of the subunits in the function of the calcium channel. *Science* **253**, 1553–1557.

SINGER–LAHAT, D., LOTAN, I., ITAGAKI, K., SCHWARTZ, A. & DASCAL, N. (1992). Evidence for the existence of BNA of Ca^{2+} channel α_2/δ subunit in *Xenopus* oocytes. *Biochimica et Biophysica Acta* **1137**, 39–44.

SOONG, T. W., STEA, A., HODSON, C. D., DUBEL, S. J., VINCENT, S. K. & SNUTCH, T. P. (1993). Structure and functional expression of a member of the low voltage-activated calcium channel family. *Science* **260**, 1193–1136.

STARR, T. V., PRYSTAY, W. & SNUTCH, T. P. (1991). Primary structure of a calcium channel that is highly expressed in the rat cerebellum. *Proceedings of the National Academy of Sciences of the USA* **88**, 5621–5625.

STEA, A., DUBEL, S. J., PRAGNELL, M., LEONARD, J. P., CAMPBELL, K. P. & SNUTCH, T. P. (1993). A β-subunit normalizes the electrophysiological properties of a cloned N-type Ca^{2+} channel α_1–subunit. *Neuropharmacology* **32**, 1103–1116.

TAKAHASHI, M., SEAGAR, M. J., JONES, J. K, REBER, B. F. X. & CATTERALL, W. A. (1987). Subunit structure of dihydropyridine-sensitive calcium channels from skeletal muscle. *Proceedings of the National Academy of Sciences of the USA* **84**, 5478–5482.

TANABE, T., TAKESHIMA, H., MIKAMI, A., FLOCKERZI, V., TAKAHASHI, H., KANGAWA, K., KOJIMA, M., MATSUO, H., HIROSE, T. & NUMA, S. (1987). Primary structure of the receptor for calcium channel blockers from skeletal muscle. *Nature* **328**, 313–318.

TOMLINSON, W. J., STEA, A., BOURINET, E., CHARNET, P., NARGEOT, J. & SNUTCH, T. P. (1993). Functional properties of a neuronal class C L-type calcium channel. *Neuropharmacology* **32**, 1117–1126.

VARADI, G., LORY, P., SCHULTZ, D., VAEADI, M. & SCHWARTZ, A. (1991). Acceleration of activation and inactivation by the β subunit of the skeletal muscle calcium channel. *Nature* **352**, 159–162.

WEI, X., PEREZ-REYES, E., LACERDA, A. E., SCHUSTER, G., BROWN, A. M. & BIRNBAUMER, L. (1991). Heterologous regulation of the cardiac Ca^{2+} channel (1 subunit by skeletal muscle β and γ subunits. *Journal of Biological Chemistry* **266**, 21943–21947.

WILLIAMS, M. E., BRUST, P. F., FELDMAN, D. H., PATTHI, S., SIMERSON, S., MAROUFI, A., MCCUE, A. F., VELICELEBI, G., ELLIS, S. B. & HARPOLD, M. M. (1992*a*). Structure and functional expression of an ω-conotoxin-sensitive human N–type calcium channel. *Science* **257**, 389-395.

WILLIAMS, M. E., FELDMAN, D. H., MCCUE, A. F., BRENNER, R., VELICELEBI, G., ELLIS, S. B. & HARPOLD, M. M. (19926). Structure and functional expression of α_1, α_2, and β subunits of a novel human neuronal calcium channel subtype. *Neuron* **8**, 71–84.

WITCHER, D. R., DE WAARD, M., SAKAMOTO, J., FRANZINI-ARMSTRONG, C., PRAGNELL, M., KAHL, S. D. & CAMPBELL, K. P. (1993). Subunit identification and reconstitution of the N-type Ca^{2+} channel complex purified from brain. *Science* **261**, 486–489.

Received 3 August 1994; accepted 8 December 1994.